JOURNAL OF BIOMEDICAL OPTICS 3(4), 391–395 (OCTOBER 1998)

INFRARED IMAGING OF *IN VIVO* MICROVASCULATURE FOLLOWING PULSED LASER IRRADIATION

Sergey A. Telenkov,[†] Derek J. Smithies,[‡] Dennis M. Goodman,[*] B. Samuel Tanenbaum,[**] J. Stuart Nelson,[‡] and Thomas E. Milner[†]

[†]The University of Texas at Austin, Biomedical Engineering Program, Austin, Texas; [‡]Beckman Laser Institute and Medical Clinic, University of California, Irvine, California; [*]Lawrence Livermore National Laboratory, University of California, Livermore, California; [**]Harvey Mudd College, Department of Engineering, Claremont, California

(Paper JBO-181 received Nov. 18, 1997; revised manuscript received May 3, 1998; accepted for publication June 2, 1998.)

ABSTRACT

Infrared emission images of the chick chorioallantoic membrane (CAM) microvasculature following pulsed laser irradiation were recorded using a high speed infrared focal plane array camera. A three-dimensional tomographic reconstruction algorithm was applied to compute the initial space-dependent temperature increase in discrete CAM blood vessels caused by light absorption. The proposed method may provide consistent estimates of the physical dimensions of subsurface blood vessels and may be useful in understanding a variety of biomedical engineering problems involving laser–tissue interaction. © *1998 Society of Photo-Optical Instrumentation Engineers.* [S1083-3668(98)00204-4]

Keywords CAM; laser; infrared imaging; FPA camera.

1 INTRODUCTION

Pulsed photothermal radiometry (PPTR) has drawn significant attention as a promising technique for noncontact material characterization. Principles and applications of pulsed photothermal radiometry for measurements of optical and thermal properties of opaque materials were developed nearly 15 years ago by Tam and co-workers.[1,2] The PPTR technique relies on detecting a transient increase in infrared radiation emitted from a light absorbing material and analysis of the subsequent temperature decay as a function of time. The recorded signal contains information concerning the sample optical absorption coefficient at the excitation wavelength, thermal diffusivity, and thickness. Numerous medical applications derived from the principles of laser photothermolysis[3] stimulated early investigations of photothermal radiometry for noncontact characterization of biological materials.[4,5] Applications of PPTR to determine the optical parameters of turbid media and the effect of light scattering on photothermal response were analyzed in a number of studies.[6,7] A review of the biological problems where PPTR provided useful information has been given by Vitkin et al.[8]

Recently, utilization of PPTR to determine dimensions of laser heated subsurface chromophores has been described by Milner et al.[9] Knowledge of the initial space-dependent temperature distribution in subsurface blood vessels in human skin immediately following pulsed laser exposure and subsequent thermal relaxation enables a clinician to optimize laser dosimetry in the clinical management of patients with port wine stain (PWS) birthmarks and other selected dermatoses.[10]

Although analysis of the temperature–time data recorded by a single-element infrared detector allows one to determine important material parameters, such an approach is essentially one dimensional. Numerous biomedical applications, however, require knowledge of the temperature increase in the lateral and longitudinal dimensions induced by absorption of pulsed laser radiation. An alternative approach to study the thermal response of biological materials is based on utilization of a focal plane array camera to record a time sequence of infrared (IR) emission images following pulsed laser irradiation. The time sequence of images may be used as input data for a tomographic reconstruction algorithm to determine the initial space-dependent temperature increase immediately following pulsed laser irradiation.

In the present study, we describe the application of an IR imaging technique to investigate temperature increase in an *in vivo* microvasculature following pulsed laser irradiation. The initial three-dimensional laser-induced temperature increase

Address all correspondence to Dr. Sergey A. Telenkov. Tel: (512) 471-4913; Fax: (512) 471-0616; E-mail: sergey@mail.utexas.edu

has been computed using an iterative reconstruction algorithm. The chick chorioallantoic membrane (CAM) provides a simple biological model to investigate the three-dimensional laser-induced temperature increase in subsurface blood vessels. The CAM vasculature is embedded in a liquid matrix transparent to visible radiation. Therefore, the CAM planar surface does not scatter incident radiation and analysis of the thermal response is simplified.

2 THEORY

A theoretical analysis of the pulsed IR imaging method and its application to reconstruct the initial space-dependent temperature increase induced by light absorption in subsurface chromophores has been given by Milner et al.[9] The time sequence of infrared images of a laser heated surface $\Delta T_S(x,y,t)$ recorded by an IR focal plane array (IR-FPA) camera is related to the initial space-dependent temperature increase $\Delta T_0(\xi,\eta,\zeta,t=0)$ in the tissue by

$$\Delta T_s(x,y,t) = \int\int_{x',y'} K_C(x-x',y-y')dx'dy' \times \int\int\int_{\xi,\eta,\zeta} K_T(x'-\xi,y' - \eta,\zeta,t)\Delta T_0(\xi,\eta,\zeta,t=0)d\xi d\eta d\zeta, \quad (1)$$

where $K_T(x'-\xi,y'-\eta,\zeta,t)$ and $K_C(x-x',y-y')$ represent, respectively, the thermal and camera point spread functions. The function K_C describes the inherent limitations of the IR-FPA camera responsible for blurring effects in the IR images. Equation (1) constitutes a forward problem in which the time sequence of infrared images may be computed from the initial space-dependent temperature increase. Inasmuch as we seek to determine the initial temperature increase immediately following pulsed laser irradiation from a time sequence of IR images, one faces an inverse problem. The integral equation of pulsed IR tomography may be written in operator form as

$$\Delta T_0(\xi,\eta,\zeta,t=0) = (K_T)^{-1}(K_C)^{-1} * \Delta T_s(x,y,t). \quad (2)$$

The tomographic Eq. (2) can be viewed as an inversion–deconvolution problem and requires a numerical algorithm to find a solution. Mathematically, Eq. (2) is an ill-posed problem due to singularities of the kernel function.[9] Analysis of different inversion methods to compute the one-dimensional initial temperature increase has been described by Milner et al.[11] Their results indicated that the initial temperature increase computed by a nonnegatively constrained conjugate-gradient algorithm was superior in terms of avoiding solution errors. This algorithm constrains the computed estimate for the initial temperature distribution to nonnegative values (i.e., $\Delta T_0 > 0$), which is consistent with the interaction of light with biological tissue.

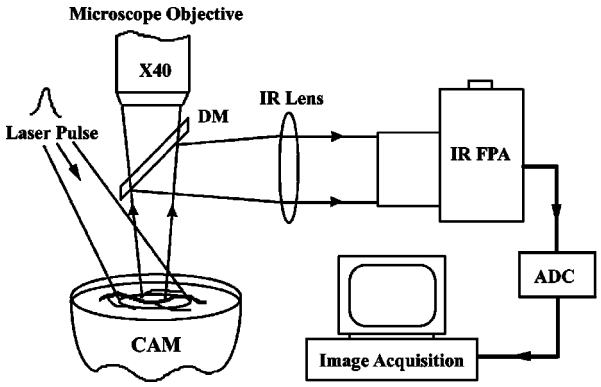

Fig. 1 Schematic of the experimental setup for pulsed infrared tomography. DM—dichroic mirror; IR FPA—infrared focal plane array; ADC—analog to digital converter.

Numerical solution of the tomographic inverse problem [Eq. (2)] is computationally intensive due to the large size of the input data. For example, a sequence of 200 images acquired by a 128 $\times$128 FPA camera represents a vector containing over 3 000 000 components. Use of the nonnegatively constrained conjugate-gradient algorithm[11,12] regularized by early termination reduces the computation time significantly. In the present study, we applied this iterative algorithm to reconstruct the three-dimensional temperature distribution [Eq. (2)] in the CAM immediately following pulsed laser irradiation.

3 EXPERIMENTAL RESULTS AND DISCUSSION

Fertilized chick eggs incubated for 11 days at 37 °C and 60% humidity were used in our experiments.[13] The egg shell apex was removed, providing access to the CAM vasculature through a 2 cm diam round window. Various investigators[13,14] have described microscopic studies of the three-dimensional spatial configuration of blood vessels in the CAM. The CAM vascular system consists of a dense network of superficial capillaries and deeper arteries and veins. Prior to laser exposure, individual blood vessels were observed under an optical microscope at 40$\times$ magnification and recorded on VHS videotape. A schematic diagram of the experimental setup is illustrated in Figure 1.

Radiation emitted by a flash-lamp pumped dye laser (Candela, model SPTL-1, Wayland, MA) with a pulse duration of 0.45 ms [full width at half maximum (FWHM)] and a wavelength of 585 nm was used to heat the CAM blood vessels. Laser output with pulse energy of 0.6–1.2 J was delivered using a 1 mm diam multimode optical fiber and a collimating lens providing an 8 mm spot diameter on the

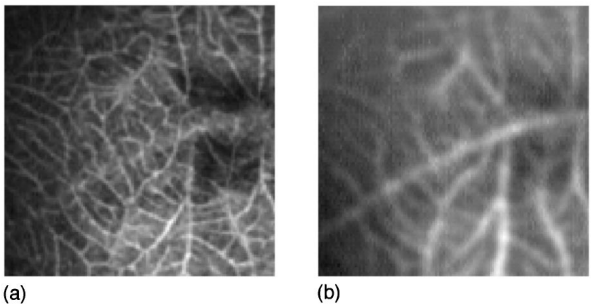

Fig. 2 Infrared images of the CAM microvasculature (a) immediately and (b) 10 ms after pulsed laser irradiation ($D=1.4\,\mathrm{J/cm^2}$, $\tau=0.45$ ms, and $\lambda=585$ nm).

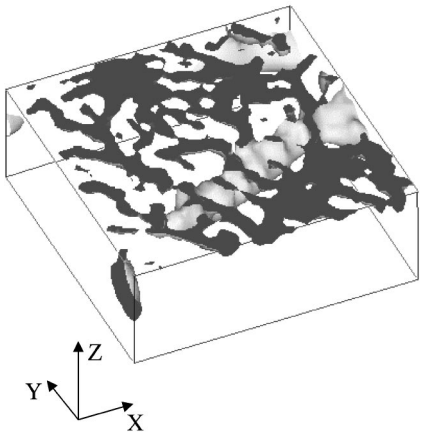

Fig. 3 Three-dimensional temperature increase in CAM blood vessels computed following laser exposure $D=1.4\,\mathrm{J/cm^2}$ ($\tau=0.45$ ms and $\lambda=585$ nm) after 10 iterations of the constrained conjugate-gradient algorithm.

CAM surface (laser fluence $D=1.2$–$2.4\,\mathrm{J/cm^2}$). A dichroic mirror (DM) with high reflectivity in the infrared spectrum (3–5 μm) was placed above the CAM surface to redirect infrared radiation from the excitation zone into the IR-FPA camera lens. An optical image of the irradiated area taken prior to laser exposure was used for microscopic measurements of the CAM blood vessels.

A time sequence of infrared emission images from the CAM surface following pulsed laser exposure was recorded by an IR-FPA camera (Amber Engineering, Galileo model, Goleta, CA), sensitive in the 3–5 μm spectral band and operating at a frame rate of 500 Hz. Application of a FPA camera for pulsed IR imaging allows the blackbody emission signal from an extended target area to be recorded following single laser exposure and provides more complete information about the specimen being studied.

Image acquisition was triggered simultaneously with laser irradiation and a sequence of 200 consecutive image frames was stored in computer random access memory for subsequent processing. The camera's IR optics provided a $4\times4\,\mathrm{mm^2}$ field of view, much smaller than the 8 mm laser irradiation spot diameter. To increase the data acquisition frame rate, the IR-FPA camera operated in a 128×128 pixel subregion readout mode, providing a lateral resolution of 30 μm/pixel. Increasing the acquisition frame rate further is possible by shrinking the imaging area.

Since CAM blood vessels are surrounded by media that are transparent in the visible spectral band, laser radiation is absorbed by hemoglobin containing red blood cells [absorption coefficient at 585 nm is $191\,\mathrm{cm^{-1}}$ (Ref. 15)] inside the CAM vasculature. An example of two selected frames from a sequence of 200 IR images acquired 10 ms apart (five frames) is shown in Figure 2. The image in Figure 2(a), recorded immediately after laser irradiation, reveals the fine structure of the superficial capillaries while the delayed emission [Figure 2(b)] image indicates that heat is generated in deeper blood vessels below the CAM surface. The recorded time sequence of the IR images was used as input data for the constrained conjugate-gradient reconstruction algorithm to compute the initial space-dependent temperature distribution within the CAM blood vessels immediately following pulsed laser irradiation. The result of the three-dimensional tomographic reconstruction of a volume below the central area of $1.9\times1.9\,\mathrm{mm^2}$ after 10 iterations is shown in Figure 3. The reconstructed image of the space-dependent initial temperature increase reveals a dense network of superficial capillaries and a larger blood vessel below the CAM surface. Camera frame rate (f) and thermal diffusivity χ of the CAM define a characteristic length $l_\chi\simeq(4\chi/f)^{1/2}$ that limits the vertical dimension of a voxel representing the initial temperature increase. With $\chi=1.4\times10^{-7}\,\mathrm{m^2/s}$ (Ref. 11) and a frame rate $f=500$ Hz, one obtains $l_\chi\simeq33$ μm. Due to this limitation, the shallow capillaries appear in the most superficial layer of voxels of the calculated initial temperature increase. The depth resolution within the superficial layer may be improved by increasing the camera frame rate, which is determined by integration and by IR-FPA readout time of the selected imaging area. For deeper blood vessels, various investigators have shown[16,17] that the spatial resolution deteriorates with increasing depth.

The computed three-dimensional temperature increase in a vertical cross section is shown in Figure 4. The maximum depth of the reconstructed temperature increase is limited by the acquisition time and by noise characteristics of the IR detection system. Heat that originates in deeper blood vessels requires a longer time to diffuse to the CAM surface. The IR-FPA camera and acquisition hardware used in the present experiments allowed us to probe the CAM vasculature to a maximum depth of 500 μm. Regions with higher temperatures in Figure 4 were visualized by choosing an appropriate color map. A substantial temperature increase after laser exposure is observed in the superficial layer

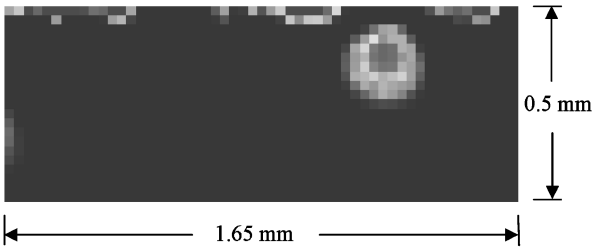

Fig. 4 Initial temperature increase in blood vessels in a plane normal to the CAM surface.

(<50 μm thick) and in a discrete large blood vessel located just beneath the CAM surface. The temperature profile along an axis passing through the large blood vessel is shown in Figure 5. The maximum temperature increase is 150 μm below the surface and may be taken as an indicator of blood vessel depth in the CAM. Meanwhile, due to the limited penetration of laser radiation ($\lambda = 585$ nm) into blood vessel, the depth measurement based on the peak initial temperature increase computed may give reduced values for sufficiently large $\mu_a d$, where μ_a is the absorption coefficient of blood at the laser excitation wavelength and d is the vessel diameter. The accuracy of the temperature reconstruction computed by the non-negatively constrained conjugate-gradient algorithm was investigated in Ref. 17 and an analysis indicated that the chromophore thickness/depth ratio had a significant effect on the computed temperature increase. For example, the analysis showed that, for a thickness/depth ratio of 50% or greater, the peak temperature increase computed can differ from the actual value by less than 20%.

From analysis of the lateral temperature profile of the computed initial temperature increase in the subsurface CAM blood vessel (Figure 4), we estimate that diameter $d = 220$ μm. Direct measurement of the same vessel through the 40× microscope objective gives $d = 185$–200 μm, which is consistent with IR data taking into account uncertainties associated with the pixel size and the characteristic thermal diffusion length.

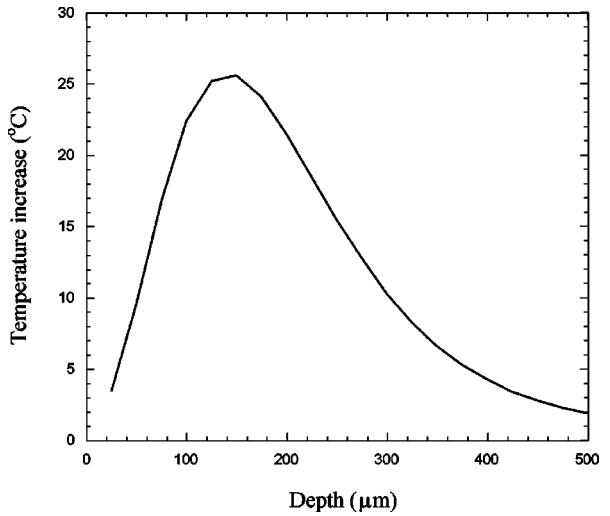

Fig. 5 Initial temperature increase vs depth along a surface normal passing through the subsurface blood vessel shown in Figure 4.

Among the possible biomedical applications of the infrared imaging method presented, noninvasive characterization of PWS vasculature has practical importance. Although the anatomy of human skin is more complicated than the simple CAM vasculature, single element PPTR measurements[10,18] have demonstrated the feasibility of mapping the laser-induced temperature increase in PWS lesions. Application of a high speed IR-FPA camera for PWS imaging may provide additional information on the laser-induced heating of subsurface blood vessels in human skin.

4 CONCLUSIONS

The laser induced temperature increase within the CAM microvasculature was studied by pulsed IR imaging. The results presented demonstrate that the initial space-dependent temperature increase in the CAM microvasculature immediately following pulsed laser irradiation can be computed using a time sequence of IR images and then applying a numerical reconstruction algorithm. Analysis of the spatial distribution of laser-induced temperature increase provides consistent estimates of the physical dimensions of subsurface blood vessels in the CAM vasculature.

Acknowledgment

This work was supported by a Biomedical Engineering Research grant (WF-21025) from the Whitaker Foundation. Support from the National Institutes of Health (RO1AR4243701A1), the Office of Naval Research (N00014-94-0874), and the Department of Energy (DE-FG03-91) is also gratefully acknowledged.

REFERENCES

1. A. C. Tam and B. Sullivan, ''Remote sensing applications of pulsed photothermal radiometry,'' *Appl. Phys. Lett.* **43**, 333–335 (1983).
2. W. P. Leung and A. C. Tam, ''Techniques of flash radiometry,'' *J. Appl. Phys.* **56**, 153–161 (1984).
3. R. R. Anderson and J. A. Parrish, ''Selective photothermolysis: Precise microsurgery by selective absorption of pulsed radiation,'' *Science* **220**, 524–527 (1983).
4. F. H. Long and T. F. Deutsch, ''Pulsed photothermal radiometry of human artery,'' *IEEE J. Quantum Electron.* **QE-23**, 1821–1826 (1987).
5. F. H. Long, N. S. Nishioka, and T. F. Deutsch, ''Measurement of the optical and thermal properties of biliary calculi using pulsed photothermal radiometry,'' *Lasers Surg. Med.* **7**, 461–466 (1987).
6. R. R. Anderson, H. Beck, U. Bruggemann, W. Farinelli, S. Jacques, and J. A. Parrish, ''Pulsed photothermal radiometry in turbid media: Internal reflection of backscattered radiation strongly influences optical dosimetry,'' *Appl. Opt.* **28**, 2256–2262 (1989).
7. S. Prahl, I. A. Vitkin, U. Bruggemann, B. C. Wilson, and R.

R. Anderson, ''Determination of optical properties of turbid media using pulsed photothermal radiometry,'' *Phys. Med. Biol.* **37**, 1203–1217 (1992).
8. I. A. Vitkin, B. C. Wilson, and R. R. Anderson, ''Pulsed photothermal radiometry studies in tissue optics,'' in *Optical-thermal Response of Laser-irradiated Tissue*, A. J. Welch and M. J. C. van Gemert, Eds., Plenum Press, New York (1995).
9. T. E. Milner, D. M. Goodman, B. S. Tanenbaum, B. Anvari, L. O. Svaasand, and J. S. Nelson, ''Imaging laser heated subsurface chromophores in biological materials: Determination of lateral physical dimensions,'' *Phys. Med. Biol.* **41**, 31–44 (1996).
10. S. L. Jacques, J. S. Nelson, W. H. Wright, and T. E. Milner, ''Pulsed photothermal radiometry of port-wine-stain lesions,'' *Appl. Opt.* **32**, 2439–2446 (1993).
11. T. E. Milner, D. M. Goodman, B. S. Tanenbaum, and J. S. Nelson, ''Depth profiling of laser-heated chromophores in biological tissues by pulsed photothermal radiometry,'' *J. Opt. Soc. Am.* **12**, 1479–1488 (1995).
12. D. M. Goodman, E. M. Johansson, and T. W. Lawrence, ''On applying the conjugate-gradient algorithm to image processing problems,'' in *Multivariate Analysis: Future Directions*, C. R. Rao, Ed., North-Holland, Amsterdam (1993).
13. S. Kimel, L. O. Svaasand, M. Hammer-Wilson, M. J. Schell, T. E. Milner, J. S. Nelson, and M. W. Berns, ''Differential vascular response to laser photothermolysis,'' *J. Invest. Dermatol.* **103**, 693–700 (1994).
14. A. Fuchs and E. S. Lindenbaum, ''The two- and three-dimensional structure of the microcirculation of the chick chorioallantoic membrane,'' *Acta Anat.* **131**, 271–275 (1988).
15. M. J. C. van Gemert, A. J. Welch, J. W. Pickering, and O. T. Tan, ''Laser treatment of port wine stains,'' in *Optical-thermal Response of Laser-irradiated Tissue*, A. J. Welch and M. J. C. van Gemert, Eds., Plenum Press, New York (1995).
16. U. S. Sathyam and S. A. Prahl, ''Limitations in measurement of subsurface temperatures using pulsed photothermal radiometry,'' *J. Biomed. Opt.* **2**, 251–261 (1997).
17. D. J. Smithies, T. E. Milner, B. S. Tanenbaum, D. M. Goodman, and J. S. Nelson, ''Accuracy of subsurface temperature distributions deduced from pulsed photothermal radiometry,'' *Phys. Med. Biol.* (in press).
18. T. E. Milner, D. J. Smithies, D. M. Goodman, A. Lau, and J. S. Nelson, ''Depth determination of chromophores in human skin by pulsed photothermal radiometry,'' *Appl. Opt.* **35**, 3379–3385 (1996).